Anamorsin/Ndor1 Complex Reduces [2Fe-2S]-MitoNEET via a Transient Protein-Protein Interaction

Anamorsin-Ndor1 complex reduces [2Fe-2S]-mitoNEET via a transient protein-protein interaction

Francesca Camponeschi[†,‡], Simone Ciofi-Baffoni[†,‡], Lucia Banci[*,†,‡]

[†]Magnetic Resonance Center (CERM), University of Florence, Via Luigi Sacconi 6, 50019, Sesto Fiorentino, Florence, Italy

[‡]Department of Chemistry, University of Florence, Via della Lastruccia 3, 50019 Sesto Fiorentino, Florence, Italy

Supporting Information

ABSTRACT: Human mitoNEET is a homodimeric protein anchored to the outer mitochondrial membrane and with a C-terminal [2Fe-2S] binding domain located in the cytosol. Recently, human mitoNEET has been shown to be implicated in Fe/S cluster repair of the cytosolic iron regulatory protein 1 (IRP1), a key regulator of cellular iron homeostasis in mammalian cells. The Fe/S cluster repairing function of mitoNEET is based on a Fe/S redox switch mechanism: under normal cellular conditions, reduced $[2Fe\text{-}2S]^{+}$ mitoNEET is present and is inactive as Fe/S cluster transfer protein; under conditions of oxidative cellular stress, the clusters of mitoNEET become oxidized and the formed $[2Fe\text{-}2S]^{2+}$ mitoNEET species reacts promptly to initiate Fe/S cluster transfer to IRP1 recycling the cytosolic apo-IRP1 into holo-aconitase. Until now, no clear data are available on which is the system reducing back the mitoNEET clusters once oxidative stress is not present anymore. In the present work we investigated, by UV-visible and NMR spectroscopies, the electron transfer process between mitoNEET and the cytosolic electron-donor Ndor1-anamorsin complex, a component of the cytosolic iron-sulfur protein assembly (CIA) machinery. The [2Fe-2S] clusters of mitoNEET are reduced via the formation of a transient complex, which brings the [2Fe-2S] clusters of mitoNEET close to the redox-active [2Fe-2S] cluster of anamorsin. Our data provide an *in vitro* evidence of a possible direct link between the CIA machinery and the mitoNEET-cluster transfer repairing pathway. This link might contribute to recover CIA machinery efficiency to mature cytosolic and nuclear Fe/S proteins.

MitoNEET is a small protein localized to the cytosolic face of the outer mitochondrial membrane by a single transmembrane helix.[1] MitoNEET forms dimers with one [2Fe-2S] cluster per monomer.[2-4] Various studies have shown that mitoNEET displays high affinity for the reduced $[2Fe\text{-}2S]^{+}$ state of the cluster, while, once oxidized, the cluster is more labile.[5-7] In-cell EPR studies showed that the [2Fe-2S] clusters of mitoNEET are in the reduced $[2Fe\text{-}2S]^{+}$ state when expressed in *E. coli* cells under normal growth conditions, and, on this basis, it was assumed to be reduced in unstressed mammalian cells.[8] This agrees with the high midpoint potential of the mitoNEET clusters, which is approximatively 0 mV at pH 7.0.[9,10] Recently, it has been proposed that mitoNEET plays a specific role in cytosolic Fe-S cluster repair of IRP1 in oxidative-stressed cells.[11] This pathway reactivates the cytosolic apo-IRP1 into Fe/S loaded, active aconitase after H_2O_2-induced oxidative and nitrosative stress, independently of the classic CIA-dependent Fe/S cluster biogenesis pathway, which matures aconitase under normal cellular conditions.[12,13] Oxidative stress conditions induce oxidation of the mitoNEET [2Fe-2S] clusters, triggering their transfer to IRP1 and transforming it in active aconitase.[11,14] Hence, mitoNEET may directly control its Fe/S cluster transfer activity via a redox switch of its redox active [2Fe-2S] clusters. While oxidative stress causes oxidation of mitoNEET clusters without their disruption,[8,15] no clear data are available on which is the protein system reducing mitoNEET clusters thus re-establishing the resting reduced state, once oxidative stress is not present anymore. Bioinformatics analysis suggested flavoproteins as possible mitoNEET reductant.[16,17] Among them, the cytoplasmic NADPH-dependent diflavin oxidoreductase 1 (Ndor1), forms a stable complex with anamorsin both *in vivo* and *in vitro*.[18-20] Anamorsin binds two [2Fe-2S] clusters in two distinct Fe/S cluster binding sites.[18,21,22] In the complex, Ndor1 reduces the [2Fe-2S] cluster bound to the first CX_8CX_2CXC motif (named redox-active cluster hereafter) of anamorsin.[18,22] The reduced cluster provides electrons for assembling cytosolic iron-sulfur cluster proteins, thus being an active player of the CIA machinery.[19] In the present work we investigated electron transfer between mitoNEET and the Ndor1-anamorsin complex by UV-visible and NMR spectroscopies. The FMN-binding domain of Ndor1 with FMN in the oxidized state (FMN-Ndor1, as obtained from the purification procedure, see Supporting Information), was first reduced anaerobically to obtain the fully reduced state of FMN with the addition of 2 equivalents of sodium dithionite. A PD-10 desalting column was then performed in order to remove any residual dithionite, and the fully reduced state of the FMN-binding domain of Ndor1 ($FMNH_2$-Ndor1) was mixed with $[2Fe\text{-}2S]^{2+}$-anamorsin at a 1:1 ratio to reduce the redox-active cluster of anamorsin ($[2Fe\text{-}2S]^{+}$-anamorsin).[18,22] Reduction of the [2Fe-2S] cluster was observed by monitoring the decrease in absorbance at 432 nm (i.e. the isosbestic point between $FMNH_2$-Ndor1 and Ndor1 with FMN in the neutral blue semiquinone state, i.e. $FMNH^{\bullet}$-Ndor1, **Figure S1**).[18] The final product upon cluster reduction is a hetero-complex formed by $FMNH^{\bullet}$-Ndor1 and $[2Fe\text{-}2S]^{+}$-anamorsin. This $FMNH^{\bullet}$-Ndor1/$[2Fe\text{-}2S]^{+}$-anamorsin complex was then mixed with oxidized $[2Fe\text{-}2S]^{2+}$-mitoNEET at a 1:1 redox-active cluster ratio, and changes in absorbance at 501 nm (the isosbestic point between $FMNH^{\bullet}$-Ndor1 and FMN-Ndor1 species, **Figure S1**) were monitored over time. The absorbance increased up to a plateau of ~0.06, indicating the occurrence of an electron transfer reaction (**Figure 1a**, **Figure S2**). At the isosbestic point of 501 nm, the oxidation of $FMNH^{\bullet}$-Ndor1 to FMN-Ndor1 does not contribute to the change in absorbance and therefore the observed increase of absorbance at 501 nm results only from the other cofactors present in the hetero-complex and in mitoNEET, i.e. the reduced $[2Fe\text{-}2S]^{+}$ cluster of anamorsin and the oxidized $[2Fe\text{-}2S]^{2+}$ clusters of mitoNEET. At the same protein concentration as that used in the electron transfer

between the FMNH•-Ndor1/[2Fe-2S]$^{+}$-anamorsin complex and [2Fe-2S]$^{2+}$-mitoNEET, the oxidation of the two [2Fe-2S]$^{+}$ clusters of anamorsin to [2Fe-2S]$^{2+}$ causes an increase in the absorbance at 501 nm of 0.26 (**Figure 1b**), and the reduction of the two [2Fe-2S]$^{2+}$ clusters of mitoNEET to [2Fe-2S]$^{+}$ causes a decrease in the absorbance at 501 nm of 0.15 (**Figure 1c**). Therefore, an overall increase in absorbance for the reduction of the two [2Fe-2S]$^{2+}$ clusters of mitoNEET by the reduced, redox-active [2Fe-2S] cluster of FMNH•-Ndor1/[2Fe-2S]$^{+}$-anamorsin complex might be expected. An experimental increase in absorbance of 0.06 at 501 nm was, indeed, observed (**Figure 1a**). However, this increase is lower than the difference expected for the reduction of the two mitoNEET clusters operated by dithionite-reduced anamorsin, which has both [2Fe-2S] clusters reduced, i.e. 0.26 minus 0.15. This lower absorbance reduction is due to the fact that, when operating with the Ndor1-anamorsin complex only the first, redox-active cluster of anamorsin is reduced. In agreement with this interpretation, by comparing the UV-visible spectra of dithionite-reduced anamorsin (**Figure 1b**, red line) with that of FMNH•-Ndor1/[2Fe-2S]$^{+}$-anamorsin complex (**Figure 1e**, orange line), it is evident that the absorption peaks at 423 and 458 nm, characteristic of the presence of anamorsin oxidized [2Fe-2S]$^{2+}$ cluster,[21,23] are still visible in the latter case, while they are bleached in the former case.

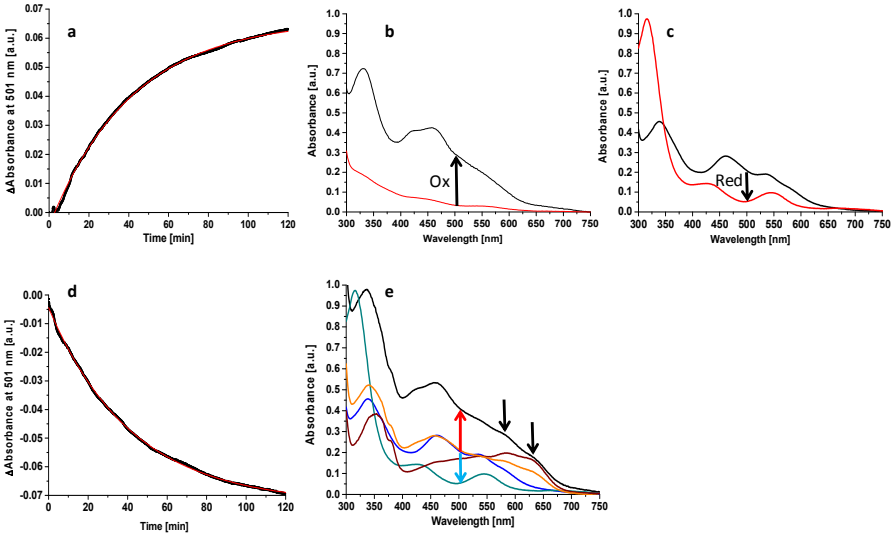

Figure 1. Reduction of [2Fe-2S]$^{2+}$ clusters of mitoNEET by the anamorsin-Ndor1 complex. (**a**) Kinetic curve of the reaction between FMNH•-Ndor1/[2Fe-2S]$^{+}$-anamorsin complex and oxidized [2Fe-2S]$^{2+}$-mitoNEET at a 1:1 ratio. The observed variation in absorbance at 501 nm was plotted as a function of time (black symbols) and fitted to a mono-exponential decay function (red line) to obtain an apparent rate constants for one-electron transfer reaction of 40 ± 1 x 10^{-5} s^{-1}. (**b**) UV-visible spectra of [2Fe-2S]$^{2+}$- (black) and [2Fe-2S]$^{+}$- (red) anamorsin. The arrow indicates the increase of absorbance at 501 nm upon oxidation (Ox) of both [2Fe-2S] clusters of anamorsin.[19,22] (**c**) UV-visible spectra of [2Fe-2S]$^{2+}$- (black) and [2Fe-2S]$^{+}$- (red) mitoNEET. The arrow indicates the decrease of absorbance at 501 nm upon reduction (Red) of the [2Fe-2S] clusters of mitoNEET. The proteins in (b) and (c) are at the same concentration used in the electron transfer reaction of (a), and were reduced with stoichiometric additions of sodium dithionite. (**d**) Kinetic curve of the reaction between FMNH•-Ndor1 and oxidized [2Fe-2S]$^{2+}$-mitoNEET at a 1:1 ratio. The observed variations in absorbance at 501 nm was plotted as a function of time (black symbols) and fitted to a mono-exponential decay function (red line) to obtain an apparent rate constants for the electron transfer reaction of 45 ± 1 x 10^{-5} s^{-1}. (**e**) UV-visible spectra of FMNH•-Ndor1/[2Fe-2S]$^{+}$-anamorsin complex mixed with [2Fe-2S]$^{2+}$-mitoNEET at a 1:1 ratio after 120 min (black), FMNH•-Ndor1/[2Fe-2S]$^{+}$-anamorsin complex before the addition of mitoNEET (orange), [2Fe-2S]$^{+}$-mitoNEET (blue), [2Fe-2S]$^{2+}$-mitoNEET (green), and FMNH•-Ndor1 (brown). The black arrows at 584 and 630 nm indicate the absorbance peaks typical of the neutral blue semiquinone state of FMN (FMNH•). The red and cyano arrows indicate the increase and decrease of absorbance at 501 nm upon oxidation of the redox-active [2Fe-2S] cluster of anamorsin and reduction of the [2Fe-2S] clusters of mitoNEET, respectively.

The data also showed that, in the FMNH•-Ndor1/[2Fe-2S]$^{+}$-anamorsin complex, the cofactor reducing mitoNEET clusters is the cluster of anamorsin, and not FMNH• of Ndor1. Indeed, if the reduction of [2Fe-2S]$^{2+}$-mitoNEET to [2Fe-2S]$^{+}$-mitoNEET were performed by the FMNH• group, a decrease of the absorbance at 501 nm would be expected (i.e. only mitoNEET clusters reduction contributes to the overall absorbance change in such case, **Figure 1c**), at variance with the increase in absorbance experimentally observed (**Figure 1a**). This is indeed what resulted by mixing FMNH•-Ndor1 with [2Fe-2S]$^{2+}$-mitoNEET at a 1:1 protein ratio where a decrease in absorbance is observed over time (**Figure 1d**, **Figure S3**). In agreement with the FMNH• group of the complex not transferring the electron to the [2Fe-2S] cluster of mitoNEET, the intense bands at 584 and 630 nm typical of FMNH•-Ndor1 are still observed once comparing the UV-visible spectrum of the final mixture with that of FMNH•-Ndor1 (**Figure 1e**, black and brown lines). On the contrary, the bands at 423 and 458 nm increase in the final mixture (**Figure 1e**, black line), because of the oxidation of the redox-active cluster of anamorsin. A simulation of the spectrum obtained in the final mixture, performed by linearly combining the UV-visible spectra of the single chromophores (i.e. FMNH•-Ndor1, [2Fe-2S]$^{2+}$-anamorsin and [2Fe-2S]$^{+}$-mitoNEET, **Figure S4**), confirms the occurrence of the electron transfer reaction between the two [2Fe-2S] clusters (eq 1):

FMNH•-Ndor1/[2Fe-2S]$^{+}$-anamorsin + [2Fe-2S]$^{2+}$-mitoNEET
↓ (1)
FMNH•-Ndor1/[2Fe-2S]$^{2+}$-anamorsin + [2Fe-2S]$^{+}$-mitoNEET

NMR spectroscopy was then used to investigate at molecular level the electron transfer process between mitoNEET and the Ndor1-anamorsin complex. The oxidized and reduced states of [2Fe-2S]-mitoNEET show different ^{1}H-^{15}N HSQC spectra (**Figure S5**), being the two species in slow exchange on the NMR time scale. Therefore, we can easily monitor the change of the cluster redox state. [2Fe-2S]$^{2+}$-mitoNEET was first titrated with FMNH•-Ndor1/[2Fe-2S]$^{+}$-anamorsin complex. When unlabeled FMNH•-Ndor1/[2Fe-2S]$^{+}$-anamorsin complex was stepwise added to ^{15}N labeled [2Fe-2S]$^{2+}$-mitoNEET up to a 1:1 redox-active cluster ratio,

a new set of backbone NH signals appeared in the ^{1}H-^{15}N HSQC map (**Figure 2a** and **2b**, **Figure S6**).

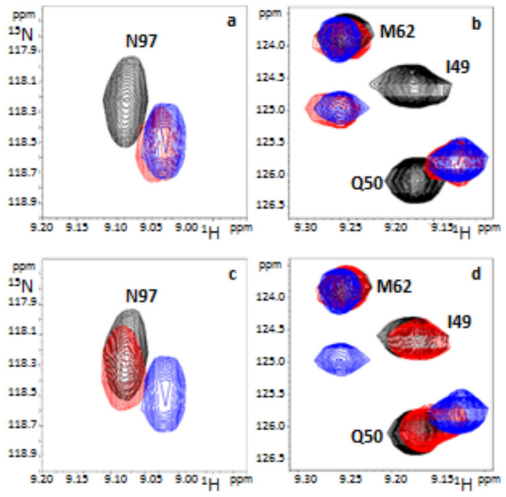

Figure 2. [2Fe-2S]-mitoNEET interacts with Ndor1-anamorsin complex. Superimposition of the ^{1}H-^{15}N HSQC spectra of $[2Fe\text{-}2S]^{2+}$-mitoNEET (black contours), $[2Fe\text{-}2S]^{+}$-mitoNEET obtained upon addition of sodium dithionite (blue contours), and $[2Fe\text{-}2S]^{2+}$-mitoNEET mixed with one equivalent of $FMNH^{\bullet}$-Ndor1/$[2Fe\text{-}2S]^{+}$-anamorsin (**a** and **b** panels, red contours), or of FMN-Ndor1/$[2Fe\text{-}2S]^{2+}$-anamorsin (**c** and **d** panels, red contours).

These signals are very close to those of $[2Fe\text{-}2S]^{+}$-mitoNEET (**Figure 2a** and **2b**), confirming the reduction of mitoNEET by $FMNH^{\bullet}$-Ndor1/$[2Fe\text{-}2S]^{+}$-anamorsin complex, as detected by UV-visible spectroscopy. However, these signals are not fully overlapped with the corresponding signals of reduced $[2Fe\text{-}2S]^{+}$-mitoNEET (**Figure 2a** and **2b**). The small differences in chemical shifts could originate from the presence of a small fraction of the complex between Ndor1-anamorsin and mitoNEET. The same titration was then performed with all proteins in their oxidized states in order to detect only protein-protein interaction effects on the NMR signals. Once unlabelled FMN-Ndor1/$[2Fe\text{-}2S]^{2+}$-anamorsin was added to oxidized ^{15}N labeled $[2Fe\text{-}2S]^{2+}$-mitoNEET up to a 1:1 redox-active cluster ratio, small chemical shift perturbations were observed for the same backbone NHs (**Figure 2c** and **2d**, **Figure S6**), indicating that [2Fe-2S]-mitoNEET weakly interacts with the Ndor1-anamorsin complex. In order to define whether both or only one component of the Ndor1-anamorsin complex interact with mitoNEET, ^{15}N-labeled mitoNEET was independently titrated with unlabeled Ndor1 and with unlabeled anamorsin. When FMN-Ndor1 was added to oxidized $[2Fe\text{-}2S]^{2+}$-mitoNEET up to 2:1 protein-protein ratio, no chemical shift variations were observed in the ^{1}H-^{15}N HSQC maps (**Figure 3a** and **3b**, **Figure S6**), indicating that no protein-protein interaction occurs between the two proteins. On the contrary, when oxidized $[2Fe\text{-}2S]^{2+}$-anamorsin was added to oxidized $[2Fe\text{-}2S]^{2+}$-mitoNEET up to 2:1 protein-protein ratio, chemical shift changes involving the same residues affected by protein-protein interaction between the FMN-Ndor1/$[2Fe\text{-}2S]^{2+}$-anamorsin complex and $[2Fe\text{-}2S]^{2+}$-mitoNEET were observed in the ^{1}H-^{15}N HSQC maps (**Figure 3c** and **3d** *vs* **Figure 2c** and **2d**, **Figure S6**), indicating the occurrence of a specific protein-protein interaction between mitoNEET and anamorsin.

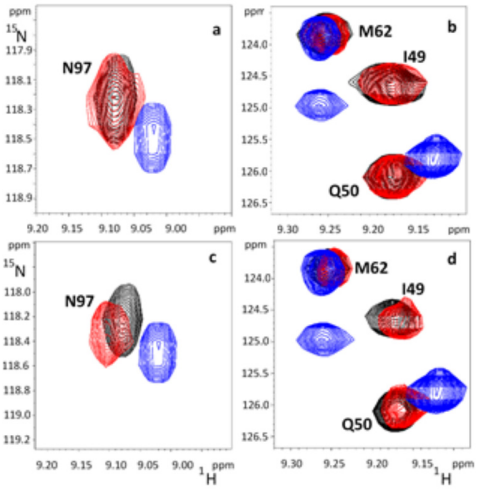

Figure 3. [2Fe-2S]-mitoNEET interacts with anamorsin and not with Ndor1. Superimposition of the ^{1}H-^{15}N HSQC spectra of $[2Fe\text{-}2S]^{2+}$-mitoNEET (black contours), $[2Fe\text{-}2S]^{+}$-mitoNEET obtained upon addition sodium dithionite (blue contours), and $[2Fe\text{-}2S]^{2+}$-mitoNEET mixed with one equivalent of FMN-Ndor1 (**a** and **b** panels, red contours), or of $[2Fe\text{-}2S]^{2+}$-anamorsin (**c** and **d** panels, red contours).

Mapping the backbone NHs chemical shift variations on the structure of [2Fe-2S]-mitoNEET, a well-defined region of interaction close to the [2Fe-2S] cluster binding site was identified, involving Ile 49, Gln 50, Lys 55, Ile 56 and Val 57 from loop L1, Glu 63 from loop L2, and Thr 94 and Asn 97 from loop L4 (**Figure 4**). Overall, the NMR data delineate a picture where $[2Fe\text{-}2S]^{+}$-anamorsin complexed with Ndor1 transfers electrons to the clusters of $[2Fe\text{-}2S]^{2+}$-mitoNEET via a transient, low populated protein-protein complex, which brings a specific region of mitoNEET containing its [2Fe-2S] clusters close to the redox-active [2Fe-2S] cluster of anamorsin.

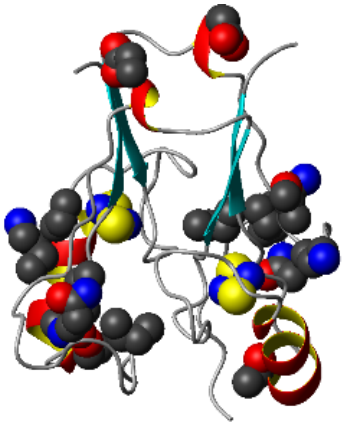

Figure 4. The region of [2Fe-2S]-mitoNEET interacting with anamorsin. The [2Fe-2S] clusters and the atoms of the residues of [2Fe-2S]-mitoNEET showing chemical shift variations upon [2Fe-2S]-anamorsin interaction are represented as spheres with conventional CPK color code on the crystal structure of [2Fe-2S]-mitoNEET (PDB ID 2QH7).

Recent studies have shown that: i) the [2Fe-2S] clusters of mitoNEET are assembled by the mitochondrial ISC assembly machinery and by the export machinery, with no apparent connection with

the CIA machinery;[11] ii) mitoNEET is an Fe/S transfer/repair system, playing such a role exclusively under conditions of oxidative stress;[11] iii) the process of cluster transfer is initiated only by changing the redox state of the mitoNEET clusters from the reduced $[2Fe\text{-}2S]^{+}$ to the oxidized $[2Fe\text{-}2S]^{2+}$ form.[7] Here, we suggest that the Ndor1-anamorsin complex, by reducing mitoNEET clusters, might act as a regulator of the termination of the cluster transfer reaction from mitoNEET to IRP1. Once oxidative stress is not present anymore, the Ndor1-anamorsin complex of the CIA machinery is formed in the cytoplasm[20] and converts back mitoNEET into its reduced $[2Fe\text{-}2S]^{+}$ form. In this way, the CIA machinery stops the mitoNEET-cluster transfer pathway to repair IRP1, as the repairing function of mitoNEET is no longer needed. This "stop" message directs both mitochondrial ISC assembly and export machineries to function exclusively for the CIA machinery. Upon mitoNEET cluster reduction, these mitochondrial machineries are, indeed, not anymore working on mitoNEET-driven IRP1 repairing pathway.[7] It is possible that a direct link between the CIA pathway and mitoNEET-cluster transfer pathway might be required to restore CIA machinery efficiency to mature cytosolic and nuclear Fe/S proteins. The present *in vitro* finding and our hypothesis of a link between these two pathways could constitute the basis for cellular studies verifying the occurrence of this connection at cellular level.

ASSOCIATED CONTENT

Supporting Information

The Supporting Information is available free of charge on the ACS Publications website.
Materials and Methods, Supplementary Figures S1-S6 (PDF)

AUTHOR INFORMATION

Corresponding Author

*banci@cerm.unifi.it

Notes

The authors declare no competing financial interests.

ACKNOWLEDGMENT

We would like to acknowledge networking support from the COST Action FeSBioNet (contract number CA15133) and financial support from the iNEXT Project 653706 "Infrastructure for NMR, EM and X-ray crystallography for translational research", both funded by the Horizon 2020 program of the European Commission.

REFERENCES

(1) Wiley, S. E.; Murphy, A. N.; Ross, S. A.; van der Geer, P.; Dixon, J. E. *Proc.Natl.Acad.Sci.USA* **2007**, *104*, 5318.
(2) Lin, J.; Zhou, T.; Ye, K.; Wang, J. *Proc.Natl.Acad.Sci.U.S.A* **2007**, *104*, 14640.
(3) Hou, X.; Liu, R.; Ross, S.; Smart, E. J.; Zhu, H.; Gong, W. *J.Biol Chem* **2007**, *282*, 33242.
(4) Paddock, M. L.; Wiley, S. E.; Axelrod, H. L.; Cohen, A. E.; Roy, M.; Abresch, E. C.; Capraro, D.; Murphy, A. N.; Nechushtai, R.; Dixon, J. E.; Jennings, P. A. *Proc.Natl.Acad.Sci.U.S.A* **2007**, *104*, 14342.
(5) Bak, D. W.; Elliott, S. J. *Biochemistry* **2013**, *52*, 4687.
(6) Zuris, J. A.; Harir, Y.; Conlan, A. R.; Shvartsman, M.; Michaeli, D.; Tamir, S.; Paddock, M. L.; Onuchic, J. N.; Mittler, R.; Cabantchik, Z. I.; Jennings, P. A.; Nechushtai, R. *Proc.Natl.Acad.Sci.U.S.A* **2011**, *108*, 13047.
(7) Golinelli-Cohen, M. P.; Lescop, E.; Mons, C.; Goncalves, S.; Clemancey, M.; Santolini, J.; Guittet, E.; Blondin, G.; Latour, J. M.; Bouton, C. *J.Biol Chem* **2016**, *291*, 7583.
(8) Landry, A. P.; Ding, H. *J.Biol Chem* **2014**, *289*, 4307.
(9) Bak, D. W.; Nechushtai, J. A.; Paddock, M. L.; Jennings, P. A.; Elliott, S. J. *Biochemistry* **2009**, *48*, 10193.
(10) Conlan, A. R.; Axelrod, H. L.; Cohen, A. E.; Abresch, E. C.; Zuris, J.; Yee, D.; Nechushtai, R.; Jennings, P. A.; Paddock, M. L. *J.Mol.Biol* **2009**, *392*, 143.
(11) Ferecatu, I.; Goncalves, S.; Golinelli-Cohen, M. P.; Clemancey, M.; Martelli, A.; Riquier, S.; Guittet, E.; Latour, J. M.; Puccio, H.; Drapier, J. C.; Lescop, E.; Bouton, C. *J.Biol.Chem.* **2014**, *289*, 28070.
(12) Stehling, O.; Mascarenhas, J.; Vashisht, A. A.; Sheftel, A. D.; Niggemeyer, B.; Rosser, R.; Pierik, A. J.; Wohlschlegel, J. A.; Lill, R. *Cell Metab* **2013**, *18*, 187.
(13) Netz, D. J.; Mascarenhas, J.; Stehling, O.; Pierik, A. J.; Lill, R. *Trends Cell Biol.* **2014**, *24*, 303.
(14) Tan, G.; Liu, D.; Pan, F.; Zhao, J.; Li, T.; Ma, Y.; Shen, B.; Lyu, J. *Biochem Biophys Res.Commun.* **2016**, *470*, 226.
(15) Landry, A. P.; Cheng, Z.; Ding, H. *Free Radic.Biol Med.* **2015**, *81*, 119.
(16) Wiley, S. E.; Paddock, M. L.; Abresch, E. C.; Gross, L.; van der Geer, P.; Nechushtai, R.; Murphy, A. N.; Jennings, P. A.; Dixon, J. E. *J.Biol Chem* **2007**, *282*, 23745.
(17) Andreini, C.; Banci, L.; Rosato, A. *J.Proteome Res.* **2016**, *15*, 1308.
(18) Banci, L.; Bertini, I.; Calderone, V.; Ciofi-Baffoni, S.; Giachetti, A.; Jaiswal, D.; Mikolajczyk, M.; Piccioli, M.; Winkelmann, J. *Proc.Natl.Acad.Sci.U.S.A* **2013**, *110*, 7136.
(19) Netz, D. J.; Stumpfig, M.; Dore, C.; Muhlenhoff, U.; Pierik, A. J.; Lill, R. *Nat.Chem.Biol.* **2010**, *6*, 758.
(20) Vernis, L.; Facca, C.; Delagoutte, E.; Soler, N.; Chanet, R.; Guiard, B.; Faye, G.; Baldacci, G. *Plos ONE* **2009**, *4*, e4376.
(21) Banci, L.; Bertini, I.; Ciofi-Baffoni, S.; Boscaro, F.; Chatzi, A.; Mikolajczyk, M.; Tokatlidis, K.; Winkelmann, J. *Chem.Biol.* **2011**, *18*, 794.
(22) Banci, L.; Ciofi-Baffoni, S.; Mikolajczyk, M.; Winkelmann, J.; Bill, E.; Eirini Pandelia, M. *J.Biol.Inorg.Chem.* **2013**, *18*, 883.
(23) Lipper, C. H.; Paddock, M. L.; Onuchic, J. N.; Mittler, R.; Nechushtai, R.; Jennings, P. A. *PLoS.One.* **2015**, *10*, e0139699.

Table of Contents artwork